Synthesis, Characterization, and Thermal Degradation Kinetics of Poly(decamethylene 2-oxoglutarate)

Fatih Doğan,[1] Hakan Akat,[2] Mehmet Balcan,[2] İsmet Kaya,[1] Mehmet Yürekli[2]

[1]*Department of Chemistry, Faculty of Arts and Science, Çanakkale Onsekiz Mart University, TR-17020, Çanakkale, Turkey*
[2]*Department of Chemistry, Faculty of Science, Ege University, Izmir, Turkey*

Received 22 March 2007; accepted 25 October 2007
DOI 10.1002/app.27570
Published online 12 February 2008 in Wiley InterScience (www.interscience.wiley.com).

ABSTRACT: Poly(decamethylene 2-oxoglutarate) [poly (DMOG)] was synthesized by a melt polycondensation reaction. The structure of poly(DMOG) was confirmed by means of Fourier transform infrared, ^{1}H-NMR, and ^{13}C NMR spectroscopies. The molecular weight distribution values of poly(DMOG) were determined with size exclusion chromatography. The number-average molecular weight, weight-average molecular weight, and polydispersity index values of poly(DMOG) were found to be 13,200, 19,000, and 1.439, respectively. Also, characterization was made by thermogravimetry (TG)–dynamic thermal analysis. The kinetics of the thermal degradation of poly (DMOG) was investigated by thermogravimetric analysis at different heating rates. TG curves showed that the thermal decomposition of poly(DMOG) occurred in one stage. The apparent activation energies of thermal decomposition for poly(DMOG), as determined by the Tang method, the Flynn–Wall–Ozawa method, the Kissinger–Akahira–Sunose method, and the Coats–Redfern method were 122.5, 126.8, 121.4, and 122.9 kJ/mol, respectively. The mechanism function and pre-exponential factor were also determined by the master plots method. J Appl Polym Sci 108: 2328–2336, 2008

Key words: activation energy; polycondensation; polyesters; thermogravimetric analysis (TGA)

INTRODUCTION

With their advantageous biodegradability potential, aliphatic polyesters have been actively studied as an alternative to some of the common synthetic polymers that cause environmental pollution problems.[1–6] The aliphatic polyesters are believed to be able to degrade easily into less harmful compounds under natural environmental conditions. However, the mechanical properties and thermal stability of these biodegradable aliphatic polyesters are not satisfactory for many industrial applications; this limits its growth in the global plastic market. New types of polymers and blends are needed that can satisfy the thermal and mechanical requirements for industrial utilization. Much research has been conducted to improve the mechanical and thermal properties and extend the applicability of aliphatic esters by physical and chemical means, such as blending and copolymerization.[7–11] Polymer blending with natural biopolymers has been used to improve the previously mentioned properties without the loss of biodegradability. Blends are preferred over copolymers in terms of their biodegradability, cost, and stability.[12–14] For example, Buchanan and coworkers[15–17] reported blends of biodegradable aliphatic polyesters and cellulose acetates (CAs). In the CA/poly(ethylene succinate) blend, the blends containing more than 70 wt % CA were found to be miscible. Biodegradation experiments on the blends revealed that poly(ethylene succinate) decomposed relatively rapidly and that CA degraded slowly. In the case of poly(tetramethylene glutarate) and poly(tetramethylene succinate)/cellulose acetate propionate (CAP) in the range of 10–40 wt % polyester, the blends had significantly higher tensile strengths, flexural moduli, and heat-deflection temperatures and greater hardness values than the corresponding CAP/dioctyl adipate blends. They also reported on a series of miscible blends consisting of CAP and poly(ethylene glutarate) or poly(tetramethylene glutarate) at a fixed CAP degree of substitution: when the content of polyester in the blend was increased, the rate of composting and the weight loss due to composting increased.

Most studies published in the literature have focused on the synthesis and relationship between the molecular structure and properties of polymers, as well as on their possible applications.[18–23] The thermal degradation of linear aliphatic polyesters was frequently investigated, and the mechanism and kinetics of their degradation have been pre-

Correspondence to: F. Doğan (fatih.dogan@ege.edu.tr).

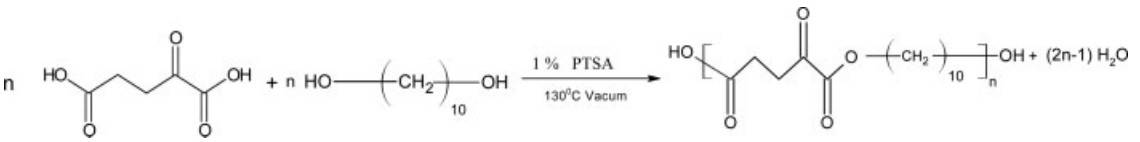

Scheme 1 Synthesis of poly(DMOG). PTSA is para toluene sulfonic acid.

sented in the literature.[24–27] The thermal decomposition processes that occur in polyesters have received continuing attention in the literature,[28–31] and due to the large number of studies carried out, one can expect that the thermal decomposition mechanism is reasonably well established. The studies done by Zimmermann[32] and McNeill and Bounekhel[33] were mainly concerned with thermal degradation at high temperatures. Passalaqua et al.[34] studied the mechanism of the thermal degradation of poly(butylene terephthalate) between 240 and 280°C and concluded that at the processing temperatures, the thermal degradation of poly(butylene terephthalate) took place at the ester linkage, as was found for the first step of poly(ethylene terephthalate) degradation.

In this study, new polyesters were synthesized and characterized to be used in applications such as polymer blending with natural polymers. Also, we attempted to determine the mechanisms of decomposition and the kinetic parameters of the synthesized polymer. The thermal degradation of the polymer was investigated by various methods of thermogravimetric analysis.

EXPERIMENTAL

Materials

All chemicals and solvents used in this study were analytical grade. The main chemicals used in this study were as follows: decamethylene glycol (Fluka, Germany, 98%), 2-oxoglutaric acid (Fluka, 98%), ethanol (Fluka, 99%), and dimethyl sulfoxide (Fluka, %99).

Synthesis of poly(decamethylene 2-oxoglutarate) [poly(DMOG)]

Poly(DMOG) was synthesized by melt polycondensation. 2-Oxoglutaric acid (10 mmol), decamethylene glycol (10 mmol), and %1 *p*-toluene sulfonic acid were used. The reaction of polycondensation was carried out under nitrogen at atmospheric pressure by the heating of the reagents first at 110–115°C for 2 h and next at 130–140°C for 6 h under reduced pressure (5 mmHg; Scheme 1). In these conditions, esterification water and excess diol were removed by distillation. The polyester obtained was a white solid.

IR (KBr): 3454 cm^{-1} (OH, the terminal groups); 2922 and 2954 cm^{-1} (aliphatic C—H stretch); 1729 cm^{-1} (C=O stretch); 1470 and 1492 cm^{-1} (C—C stretch); 1282, 1186, and 1101 cm^{-1} (C—O—C stretch). ^{1}H-NMR [deuterated chloroform ($CDCl_3$), δ]: 4.24 ppm (t 2H, COO—O—CH_2), 4.06 ppm (t 2H, O—CH_2—CH_2), 3.13 ppm (t 2H, CH_2—CO—CO—CH_2), 2.63 ppm (t 2H, CO—CH_2—CH_2), 1.73–1.360 (m 12H, H_2C—CH_2). ^{13}C-NMR ($CDCl_3$, δ): 192.84, 172.27, and 160.89 ppm (C=O); 66.81 and 65.29 ppm (O—CH_2); 34.45 ppm (CO—CH_2); 28.74 ppm (COO—CH_2); 29.81, 29.57, 29.54, 29.38, 28.54, 27.84, 26.03, and 25.92 ppm (H_2C—CH_2).

Measurements

^{1}H-NMR and ^{13}C-NMR spectra were recorded on Varian AS-400 spectrometers in $CDCl_3$. Fourier transform infrared (FTIR) spectra were obtained with a PerkinElmer spectrophotometer. The number-average molecular weight, weight-average molecular weight, and polydispersity index values were determined by a Shimadzu size exclusion chromatograph (Japan). For size exclusion chromatography investigations, we used SGX (100 Å and 7 mm diameter loading material) 7.7-mm diameter × 300-mm columns. The eluent was dimethylformamide (0.4 mL/min), and we used polystyrene standards (Polymer Laboratories, Germany). A refractive-index detector (at 25°C) was used to analyze the poly(DMOG). The thermogravimetry (TG) curves were obtained with a Shimadzu TGA-50 thermobalance. The measurements were performed with a dynamic nitrogen furnace atmosphere at a flow rate of 60 mL/min up to 1000°C. The heating rates (β's) were 5, 10, 15, and 20°C/min, and the sample sizes ranged in mass from 8 to 10 mg. A platinum crucible was used as a sample container.

Kinetic methods

The application of dynamic thermogravimetry (DTG) methods holds great promise as a tool for unraveling the mechanisms of physical and chemical processes that occur during polymer degradation. In this study, integral isoconversional methods were used to analyze the nonisothermal kinetics of poly (DMOG).

TABLE I
Algebraic Expressions for the Most Frequently Used Mechanisms of a Solid-State Process

No.	Mechanisms	Symbol	Differential form: $f(\alpha)$	Integral form: $g(\alpha)$
Deceleration curves				
1	Diffusion, 1D	D_1	$1/(2\alpha)$	α^2
2	Diffusion, 2D	D_2	$1/[\ln(1-\alpha)]$	$(1-\alpha)\ln(1-\alpha)+\alpha$
3	Diffusion, 3D	D_3	$1.5/[(1-\alpha)^{-1/3}-1]$	$(1-2\alpha/3)-(1-\alpha)^{2/3}$
4	Diffusion, 3D	D_4	$[1.5(1-\alpha)^{2/3}][1-(1-\alpha)^{1/3}]^{-1}$	$[1-(1-\alpha)^{1/3}]^2$
5	Diffusion, 3D	D_5	$(3/2)(1+\alpha)^{2/3}[(1+\alpha)^{1/3}-1]^{-1}$	$[(1+\alpha)^{1/3}-1]^2$
Sigmoidal curves				
6	N and G (n = 1)	A_1	$(1-\alpha)$	$[-\ln(1-\alpha)]$
7	N and G (n = 1.5)	$A_{1.5}$	$(3/2)(1-\alpha)[-\ln(1-\alpha)]^{1/3}$	$[-\ln(1-\alpha)]^{2/3}$
8	N and G (n = 2)	A_2	$2(1-\alpha)[-\ln(1-\alpha)]^{1/2}$	$[-\ln(1-\alpha)]^{1/2}$
9	N and G (n = 3)	A_3	$3(1-\alpha)[-\ln(1-\alpha)]^{2/3}$	$[-\ln(1-\alpha)]^{1/3}$
10	N and G (n = 4)	A_4	$4(1-\alpha)[-\ln(1-\alpha)]^{3/4}$	$[-\ln(1-\alpha)]^{1/4}$
11	Contracted geometry shape (cylindrical symmetry)	R_2	$3(1-\alpha)^{2/3}$	$1-(1-\alpha)^{1/3}$
12	Contracted geometry shape (sphere symmetry)	R_3	$3(1-\alpha)^{2/3}$	$1-(1-\alpha)^{1/3}$
Acceleration curves				
13		P_1	1	α
14		P_2	$2\alpha^{1/2}$	$\alpha^{1/2}$
15		P_3	$(1.5)\alpha^{2/3}$	$\alpha^{1/3}$
16		P_4	$4\alpha^{3/4}$	$\alpha^{1/4}$
17		$P_{3/2}$	$2/3(\alpha)^{-1/2}$	$\alpha^{3/2}$
18		$P_{2/3}$	$3/2(\alpha)^{1/3}$	$\alpha^{2/3}$
19		$P_{3/4}$	$4/3(\alpha)^{-1/3}$	$\alpha^{3/4}$

1D, one-dimensional diffusion; 2D, two-dimensional diffusion; 3D, three-dimensional diffusion; N, nucleation; G, growth.

The rate of solid-state nonisothermal decomposition reactions is expressed as

$$\frac{d\alpha}{dT}=\left(\frac{A}{\beta}\right)\exp\left(\frac{-E}{RT}\right)f(\alpha) \tag{1}$$

where T is absolute temperature (K), A is the pre-exponential factor (min^{-1}), E is the activation energy (kJ/mol), R is the gas constant (8.314 J mol^{-1} K^{-1}). Rearranging eq. (1) and integrating both sides of the equation leads to the following expression

$$g(\alpha)=\left(\frac{A}{\beta}\right)\int_{T_0}^{T}\exp\left(\frac{-E}{RT}\right)dT=\left(\frac{AE}{\beta R}\right)p(u) \tag{2}$$

where T_0 is taken as 0K for convenience of achieving the temperature integral, $p(u)=\int_{\infty}^{u}-\left(e^{-u}/u^2\right)du$ and $u=E/RT$.

Flynn–Wall–Ozawa (FWO) method[35,36]

This method was derived from the integral method. The technique assumes that A, function of conversion $f(\alpha)$, and E are independent of T, whereas A and E are independent of the degree of conversion (α). Equation (2) may then be integrated to give the following in logarithmic form:

$$\log g(\alpha)=\log(AE/R)-\log\beta+\log p(E/RT) \tag{3}$$

where $g(\alpha)$ is the integral function of conversion and p is the integral function. With Doyle's approximation[37] for the integral, which allows for $E/RT>20$, eq. (3) now can be simplified as

$$\log\beta=\log(AE/R)-\log g(\alpha)-2.315-0.4567\,E/RT \tag{4}$$

Coats–Redfern (CR) method[38]

The CR method is also an integral method, and it involves the thermal degradation mechanism. With an asymptotic approximation for resolution of eq. (2), the following equation can be obtained:

$$\ln\left(\frac{g(\alpha)}{T^2}\right)=\ln\left(\frac{AR}{E\beta}\right)-\frac{E}{RT} \tag{5}$$

The expressions of $g(\alpha)$ for the different mechanisms are listed in Table I,[39,40] and E for the degradation mechanism can be obtained from the slope of a plot of $\ln[g(\alpha)/T^2]$ versus $1000/T$.

Tang (TM) method[41]

With the logarithms of side taken and an approximation formula for the solution of eq. (2) used, the following equation can be obtained:

$$\ln\left(\frac{\beta}{T^{1.894661}}\right)=\ln\left(\frac{AE}{R\,g(\alpha)}\right)+3.635041-1.894661\ln E-\frac{1.001450E}{RT} \tag{6}$$

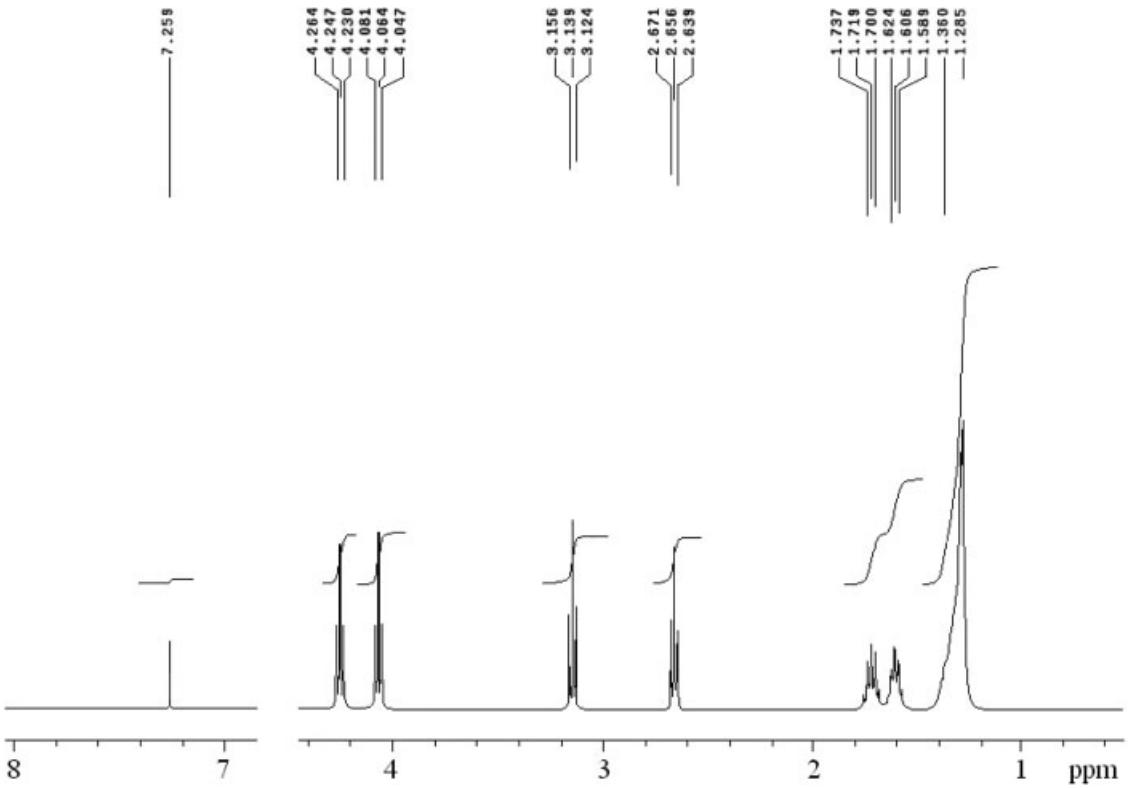

Figure 1 ^{1}H-NMR spectrum of poly(DMOG).

The plots of $\ln(\beta/T^{1.894661})$ versus $1/T$ give a group of straight lines. E can be obtained from the slope $-1.001450\ E/R$ of the regression line.

Kissinger–Akahira–Sunose (KAS) method[42]

This method is an integral isoconversional method similar to the FWO method.

$$\ln\left[\frac{\beta}{T^2}\right] = \ln\left[\frac{AR}{E\,g(\alpha)}\right] - \frac{E}{RT} \tag{7}$$

The dependence of $\ln(\beta/T^2)$ on $1/T$ calculated for the same α value at different β's can be used to calculate E.

Determination of the kinetic model by the master plot method

With a reference at point $\alpha = 0.5$ and according to eq. (2), one gets

$$g(\alpha) = \left(\frac{AE}{\beta\,R}\right)p(u_{0.5}) \tag{8}$$

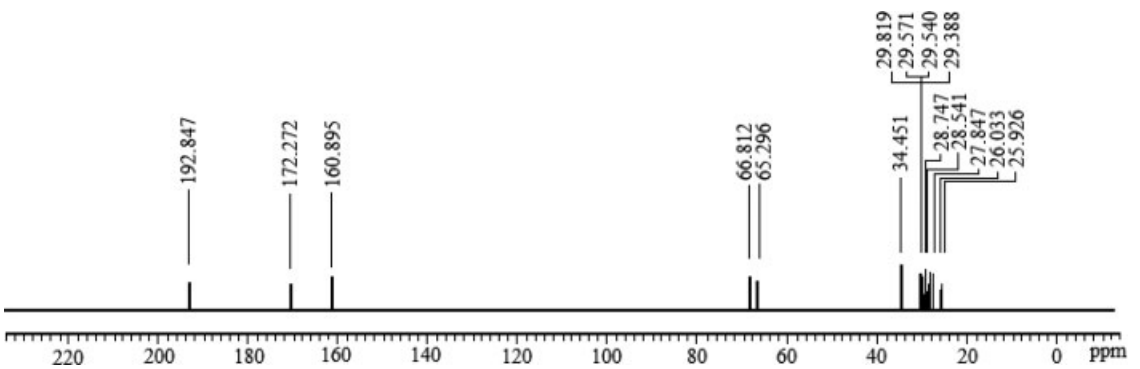

Figure 2 ^{13}C-NMR spectrum of poly(DMOG).

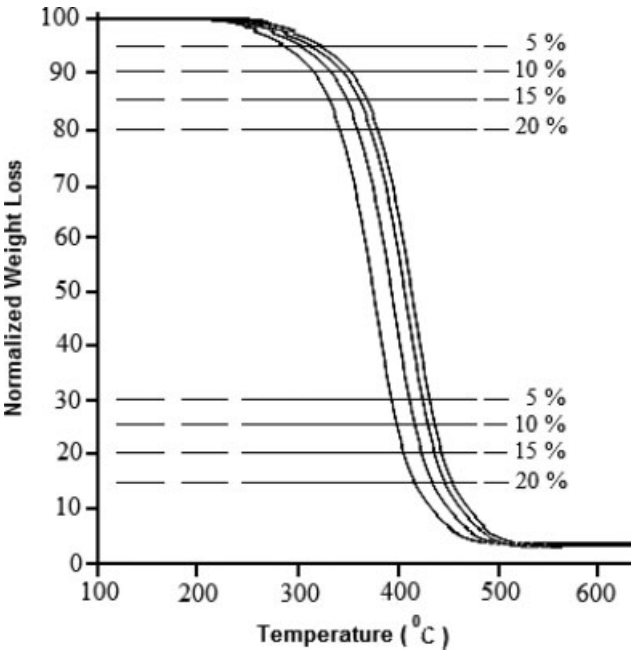

Figure 3 TG curves of poly(DMOG).

where $u_{0.5} = E/RT$. When eq. (2) is divided by eq. (8), the following equation is obtained

$$\frac{g(\alpha)}{g(0.5)} = \frac{p(u)}{p(u_{0.5})} \tag{9}$$

Plots of $g(\alpha)/g(0.5)$ against α correspond to theoretical master plots of various $g(\alpha)$ functions.[43,44] To draw the experimental master plots of $p(u)/p(u_{0.5})$ against α from experimental data obtained under different β's, an approximate formula[45] of $p(u)$ with high accuracy was used $p(u) = \exp(-u)/[u(1.00198882u + 1.87391198)]$. Equation (9) indicates that for a given α, the experimental values of $g(\alpha)/g(\alpha_{0.5})$ are equivalent when an appropriate kinetic model is used. Comparing the experimental master plots with the theoretical ones, one can determine the kinetic model.[46]

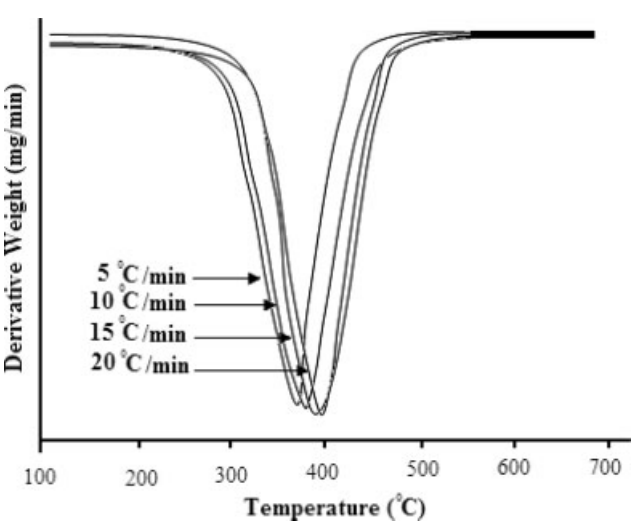

Figure 4 DTG curves of poly(DMOG).

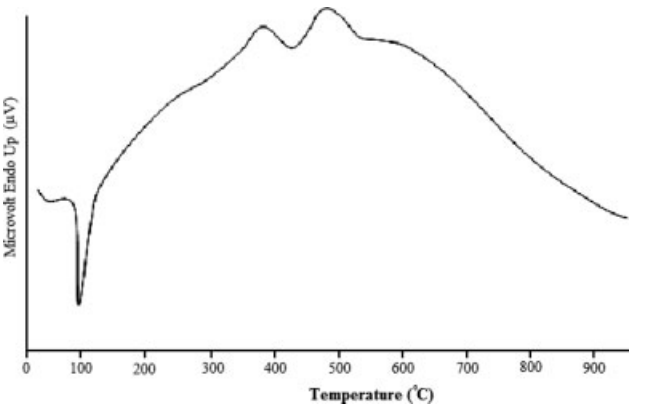

Figure 5 DTA curves of poly(DMOG).

RESULTS AND DISCUSSION

Poly(DMOG) was prepared according to Scheme 1. The characterization was confirmed by FTIR, ^{1}H-NMR, and ^{13}C-NMR spectra, which are given in Figures 1 and 2. The characteristic FTIR absorption band for the C=O ester group at 1729 cm^{-1} was very strong. A weak band at about 2922 and 2954 cm^{-1} was attributed to C—H stretching. The broad bands at 3454 cm^{-1}, with a medium intensity, proved the presence of the terminal hydroxyl groups. Poly(DMOG) also exhibited two characteristic bands at 1470 and 1492 cm^{-1} due to C—C stretching. The polyester exhibited three bands at 1282, 1186, and 1101 cm^{-1}, which were all attributed to C—O stretching. ^{1}H-NMR spectroscopy showed peaks at 4.24 ppm (t 2H, COO—O—CH_2), 4.06 ppm (t 2H, O—CH_2—CH_2), 3.13 ppm (t 2H, CH_2—CO—CO—CH_2), 2.63 ppm (t 2H, CO—CH_2—CH_2), and 1.73–1.360 ppm (m 12H, H_2C—CH_2). Also,

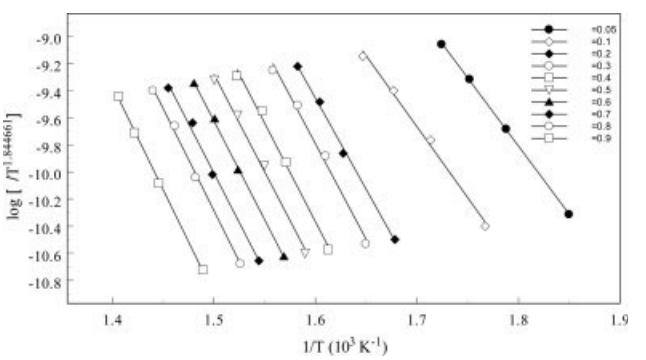

Figure 6 TM method plots of poly(DMOG) decomposition at various α's in N_2.

TABLE II
***E* Values of Poly(DMOG) Decomposition Obtained by the TM, KAS, and FWO Methods**

	TM method		KAS method		FWO method	
α	*E* (kJ/mol)	*r*	*E* (kJ/mol)	*r*	*E* (kJ/mol)	*r*
0.05	82.10	0.99629	81.56	0.99624	86.45	0.99704
0.10	81.20	0.99569	80.64	0.99564	86.00	0.99664
0.15	87.72	0.99533	87.19	0.99528	92.40	0.99624
0.20	98.81	0.99684	98.27	0.99684	103.1	0.99744
0.25	109.2	0.99297	108.6	0.99287	113.1	0.99413
0.30	116.9	0.99579	116.4	0.99574	120.5	0.99649
0.35	125.2	0.99634	124.6	0.99629	128.5	0.99689
0.40	126.0	0.99468	125.4	0.99463	129.3	0.99548
0.45	124.2	0.99357	123.6	0.99352	127.7	0.99458
0.50	126.7	0.99408	126.1	0.99403	130.2	0.99498
0.55	121.2	0.99433	120.6	0.99428	125.0	0.99523
0.60	129.9	0.99899	129.3	0.99899	133.4	0.99944
0.65	132.3	0.99483	131.8	0.99478	135.8	0.99564
0.70	133.7	0.99513	133.1	0.99508	137.1	0.99584
0.75	144.8	0.99181	144.2	0.99176	147.8	0.99297
0.80	152.3	0.99181	151.7	0.99176	155.0	0.99287
0.85	142.1	0.99453	141.5	0.99448	145.4	0.99533
0.90	161.4	0.99307	160.8	0.99302	163.9	0.99398
0.95	131.9	0.99378	131.2	0.99368	136.0	0.99473
Mean	122.5		121.4		126.8	

r = correlation coefficient of the linear plots.

^{13}C-NMR showed that the peaks at 192.84, 172.27, and 160.89 ppm corresponded to the carbonyl carbon. Eight aromatic carbon peaks between 25.92 and 29.81 ppm corresponded to the eight equivalent carbon atoms from the aliphatic chain, whereas those at 66.81 and 65.29 ppm corresponded to the methyl group of poly(DMOG).

Thermal decomposition process

The thermal decomposition of poly(DMOG) was selected for the kinetic study. *E* of the decomposition process was determined by multiple β kinetics. Typical DTG and differential thermal analysis (DTA) thermograms of poly(DMOG) in a dynamic nitrogen atmosphere are shown in Figures 3–5, where the TG curves are the decomposition of 8–10-mg poly (DMOG) samples at rates of 5, 10, 15, and 20°C/min under a nitrogen flow of 60 mL/min. All TG curves of poly(DMOG) showed that thermal decomposition took place mainly in one stage. From the corresponding DTG profiles, the temperatures related to the maximum decomposition rates were found to be 364, 383, 393, and 400°C.

Determination of *E*

Several techniques with different approaches have been developed to solve the integral of eq. (2). The four methods investigated in this study were those of the FWO, KAS, TM, and CR methods. The CR method is based on a single β, whereas the other methods are based on multiple β's. First, isoconver-

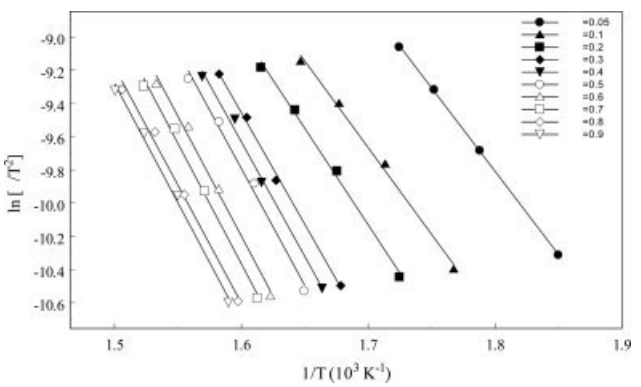

Figure 7 KAS plots of poly(DMOG) decomposition at various α's in N_2.

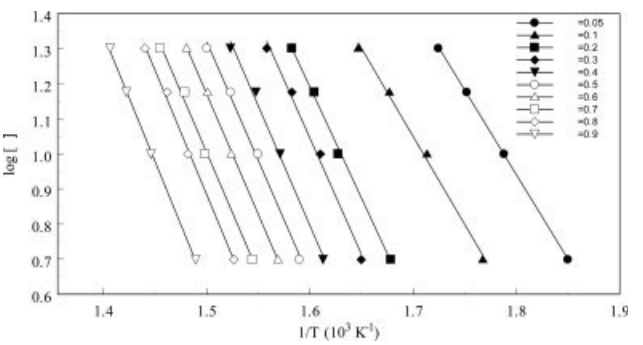

Figure 8 FWO plots of poly(DMOG) decomposition at various α's in N_2.

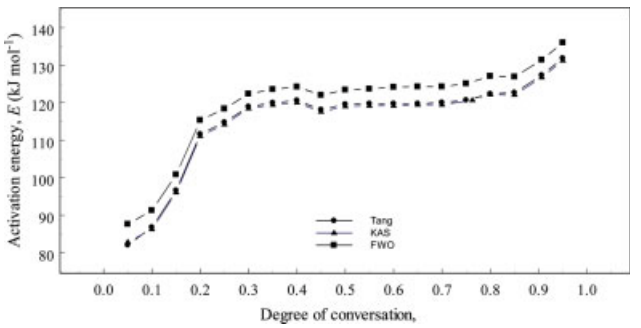

Figure 9 E as a function of α for the decomposition process of poly(DMOG) calculated by the TM, KAS, and FWO methods. [Color figure can be viewed in the online issue, which is available at www.interscience.wiley.com.]

sional methods were applied to analyze the TG data of poly(DMOG) because it is independent of any thermodegradation mechanisms. Equation (6) was used to obtain E, which could be calculated from the plot of ln $(\beta/T^{1.894661})$ versus $1000/T$ fit to a straight line (shown in Fig. 6). The mean value of the E of the thermal degradation of poly(DMOG) in N_2 was 122.5 kJ/mol. The calculated results are summarized in Table II.

Another isoconversion method used in this article was that of KAS. Equation (7) was used to determine the values of E from plots of $\ln(\beta/T^2)$ against $1000/T$ over a wide range of α (shown in Fig. 7). In this case, the range $\alpha = 0.05$–0.95 was chosen to evaluate the E values of poly(DMOG). The determined E values are listed in Table II, and the average value for the thermal degradation of poly(DMOG) was 121.4 kJ/mol over the given range of α. This result agreed well with the mean value of E obtained by the TM method.

The FWO method is an integral method also independent of the degradation mechanism. Equation (4) was used, and the apparent E of poly(DMOG) could, therefore, be obtained from a plot of log β against $1000/T$ for a fixed α because the slope of such a line is given by $-0.456E/RT$. Figure 8 illustrates the plots of ln β versus $1000/T$ at various α's. The E values calculated from the slopes are tabulated in Table II, and the mean values of E were determined to be 126.8 kJ/mol; comparatively, the E value of poly (DMOG) was very close to the values obtained by the two methods. The E values of poly(DMOG) obtained by the TM, FWO, and KAS methods were 125.5, 126.8, 121.4 kJ/mol, respectively.

Constant mass loss lines were determined by the measurement of the temperature at a given mass percentage for each rate. In Figures 6–8, the Arrhenius-type plots of DTG runs for the decomposition of poly(DMOG) are shown for masses ranging from $\alpha = 0.1$ to 0.95 in N_2. Table II summarizes the effect of E and correlation coefficient values on the overall mass loss from 5 to 95 mass % in N_2. The thermal decomposition of poly(DMOG) in N_2 presented similar behavior for the TM, KAS, and FWO methods (shown in Fig. 9). The initial E required for initial decomposition was approximately 85 kJ/mol. The E values for poly(DMOG) in the region $0.2 < \alpha < 0.85$ were very close. The values of E versus α are shown in Figure 9. For the region of $\alpha = 0.2$–0.85, little dependence of E on α was observed, which indicated

TABLE III
E Values of Poly(DMOG) Decomposition in an Atmosphere of N_2 as Obtained by the CR Method

	5°C/min		10°C/min		15°C/min		20°C/min	
	E (kJ/mol)	r	E (kJ/mol)	r	E (kJ/mol)	r	E (kJ/mol)	r
A_1	76.99	0.99761	83.52	0.99598	88.97	0.99599	92.69	0.99507
$A_{1.5}$	47.93	0.99709	52.24	0.99556	55.75	0.99548	58.18	0.99507
A_2	33.47	0.99678	36.54	0.99505	39.14	0.99485	40.92	0.99382
A_3	18.87	0.99587	20.87	0.99364	22.53	0.99309	23.67	0.99195
A_4	11.61	0.99433	13.07	0.99133	14.23	0.99022	15.04	0.98901
D_1	118.5	0.99258	128.3	0.99143	135.4	0.97816	141.3	0.98054
D_2	130.8	0.99345	141.5	0.99215	149.6	0.98627	156.1	0.98766
D_3	136.2	0.99538	147.1	0.99407	155.7	0.98923	162.2	0.99021
D_4	146.7	0.99761	158.7	0.99811	168.2	0.99348	175.1	0.99368
D_5	107.7	0.98334	116.6	0.98748	122.9	0.99322	128.4	0.97592
R_2	64.35	0.99549	69.89	0.99404	74.19	0.98909	77.46	0.99006
R_3	68.28	0.99720	74.12	0.99574	78.77	0.99243	82.18	0.99275
P_1	54.19	0.98465	58.95	0.98349	62.37	0.97392	65.27	0.97684
P_2	22.05	0.97551	24.25	0.97463	25.84	0.96113	27.21	0.96592
P_3	11.27	0.95705	12.68	0.95771	13.67	0.93787	14.53	0.94638
P_4	5.917	0.96609	6.602	0.97313	7.582	0.94495	8.192	0.90733
$P_{3/2}$	86.38	0.98666	93.64	0.98553	98.93	0.97689	103.3	0.97940
$P_{2/3}$	32.73	0.98080	35.81	0.97971	38.02	0.96839	39.94	0.97184
$P_{3/4}$	38.13	0.98221	41.67	0.98109	44.11	0.98109	46.24	0.97382

r = correlation coefficient of the linear plots.

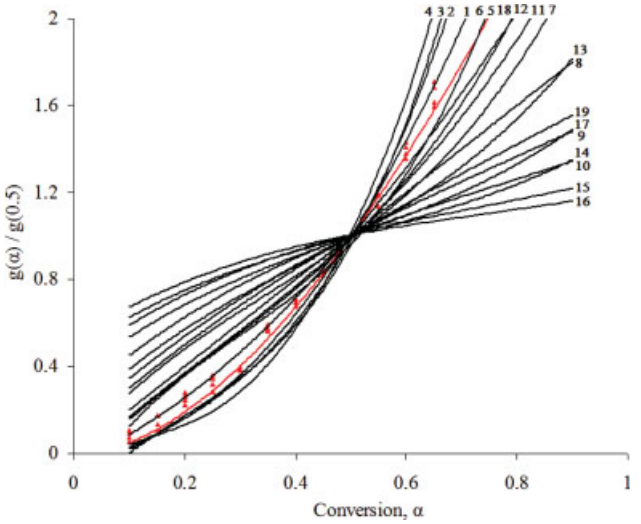

Figure 10 Master plots of theoretical $g(\alpha)/g(0.5)$ against α for various reaction models (the solid curves represent the 19 kinds of reaction models given in Table I) and (▲) experimental data for the decomposition of poly(DMOG) at β's of 5, 10, 15, and 20°C/min. [Color figure can be viewed in the online issue, which is available at www.interscience.wiley.com.]

that there existed a high probability for the presence of a single-step reaction.[47] Therefore, this allowed us to estimate the most probable kinetic model. To find out the mechanism of the thermal decomposition of poly(DMOG), the CR method was chosen, as it involves the mechanisms of a solid-state process. According to eq. (5), the E for every $g(\alpha)$ function listed in Table I can be calculated at constant β's from the fitting of $\ln[g(\alpha)/T^2]$ versus $1000/T$ plots. The E values and the correlation coefficients at constant β's of 5, 10, 15, and 20°C/min are tabulated in Table III for the thermal degradation of poly

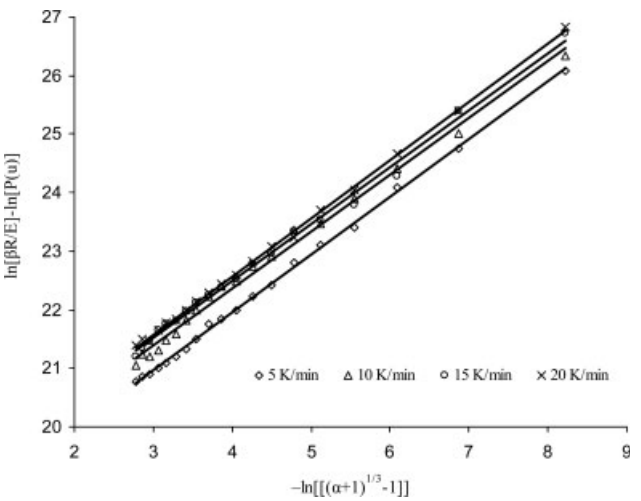

Figure 11 Plot of $\ln(\beta R/E) - \ln[p(u)]$ versus $-\ln\{[(1+\alpha)^{1/3}] - 1\}$ for poly(DMOG) decomposition at various β's.

TABLE IV
***E* Values and Correlation Coefficients Obtained by the Plotting of $\ln(\beta R/E) - \ln[p(u)]$ Versus $-\ln\{[(1+\alpha)^{1/3}] - 1\}$**

β (K/mol)	ln A (s^{-1})	r
5	18.07	0.99949
10	18.49	0.99659
15	18.59	0.99779
20	18.59	0.99954
Mean	18.43	

r = correlation coefficient of the linear plots.

(DMOG). Especially at a β of 15°C/min for the decomposition stage of poly(DMOG), the E corresponding to mechanism D_5 was 122.9 kJ/mol, which was very close to the value of 122.5 kJ/mol obtained by the TM method. The correlation coefficient was also much higher than the others. To confirm the conclusions, the experimental master plots of $g(u)/g(u_{0.5})$ against α constructed from experimental data of the thermal decomposition of poly(DMOG) under different β's and the theoretical master plots of various kinetic functions are all shown in Figure 10. The comparisons of the experimental master plots with theoretical ones indicated that the kinetic process of the thermal decomposition of poly(DMOG) agreed with the D_5 master curve for the decomposition stage very well. With the assumption of deceleration α-time curves (D_n) law, the experimental data, the expression of the D_n model, and the average reaction energy predetermined were introduced into eq. (2), and the following expression was obtained:

$$\ln[\beta R/E] - \ln[p(u)] = \ln A - \ln\{[(1+\alpha)^{1/3}] - 1\} \quad (10)$$

We obtained a group of lines by plotting $\ln(\beta R/E) - \ln[p(u)]$ against $-\ln\{[(1+\alpha)^{1/3}] - 1\}$. As shown in Figure 11 and Table IV, A was calculated from the intercepts of the lines corresponding to various β's and was found to be 18.43 s^{-1}.

CONCLUSIONS

A new polyester, poly(DMOG), was synthesized and was characterized by FTIR, ^{1}H-NMR, ^{13}C-NMR, and TG–DTA techniques. The number-average molecular weight, weight-average molecular weight, and polydispersity index values of poly(DMOG) were found to be 13,200, 19,000, and 1.439, respectively. Poly (DMOG) exhibited two-step decomposition processes in the DTA profile. The exothermic thermal effect at 366 K corresponded to the melting point of poly (DMOG). The second exothermic peak was due to the decomposition of poly(DMOG). The kinetics of the thermal degradation of poly(DMOG) were investigated by thermogravimetric analysis at different

β's. The *E* values of the thermal degradation of poly(DMOG) in N_2 obtained by the TM, KAS, FWO, and CR methods were 122.5, 126.8, 121.4, and 122.9 kJ/mol, respectively, for the decomposition stage. The analysis of the results obtained by the CR method and master plots method showed that the degradation mechanism of poly(DMOG) in N_2 went to the D_5 mechanism for the decomposition stage.

References

1. Doi, Y.; Tamaki, A.; Kunioka, M.; Soga, K. Appl Microbiol Biotechnol 1988, 28, 330.
2. Lee, S. H.; Ohkita, T. Holzforschung 2004, 58, 537.
3. Qiu, Z.; Komura, M.; Ikehara, T.; Nishi, T. Polymer 2003, 44, 7749.
4. Albertsson, A. C.; Lungguist, O. J. J Macromol Sci Chem 1986, 23, 393.
5. Tokiwa, Y.; Suzuki, T. J Appl Polym Sci 1981, 26, 441.
6. Tokiwa, Y.; Suzuki, T. J Polym Sci Polym Lett Ed 1981, 19, 159.
7. Fredericks, R. J.; Melveger, A. J.; Colegiewitz, L. J. J Polym Sci Polym Phys Ed 1984, 22, 57.
8. Albertsson, A. C.; Lungguist, O. J. J Macromol Sci Chem 1986, 23, 411.
9. Albertsson, A. C.; Lungguist, O. J. J Macromol Sci Chem 1987, 24, 977.
10. Zhang, Y.; Feng, Z. G.; Wu, T.; Zhang, A. Y. Acta Polym Sinica 2003, 6, 776.
11. Nugroho, P.; Mitomo, H.; Yoshii, H.; Kume, T.; Nishimura, K. Macromol Mater Eng 2001, 5, 286.
12. Ogata, N.; Kinari, T.; Kumagai, S.; Yanagawa, T.; Ogihara, T.; Yoshida, N. Sen-I Gakkaishi 1996, 52, 277.
13. Ueaska, T.; Ogata, N.; Nakane, K.; Ogihara, T. Sen-I Gakkaishi 2002, 58, 437.
14. Chong, K. F.; Schmidt, H.; Kummerlowe, C.; Kamer, H. W. J Appl Polym Sci 2000, 92, 149.
15. Buchanan, C. M.; Pearcy, B. G.; White, A. W.; Wood, M. D. J Environ Polym Degrad 1997, 5, 209.
16. Buchanan, C. M.; Boggs, C. N.; Dorschel, D. D.; Gardner, R. M.; Komarek, R. J.; Watterson, T. L.; White, A. W. J Environ Polym Degrad 1995, 3, 1.
17. White, A. W.; Buchanan, C. M.; Pearcy, B. G.; Wood, M. D. J Appl Polym Sci 1994, 52, 525.
18. Burchard, W. Adv Polym Sci 1999, 143, 113.
19. Haag, R.; Vogtle, F. Angew Chem 2004, 116, 274.
20. Mecking, S.; Thormann, R.; Frey, H.; Sunder, A. Macromolecules 2000, 33, 3958.
21. Pirrung, F. O. H.; Loen, E. M.; Noordam, A. Macromol Symp 2002, 187, 683.
22. Stiriba, S. E.; Frey, H.; Haag, R. Angew Chem 2002, 114, 1385.
23. Ballauff, M. Top Curr Chem 2001, 212, 177.
24. Kricheldorf, H. R.; Luderwald, I. Makromol Chem 1978, 179, 421.
25. Kopinke, F. D.; Remmler, M.; Mackenzie, K. Polym Degrad Stab 1996, 52, 25.
26. Persenaire, O.; Alexandre, M.; Degeé, P.; Dubois, P. Biomacromolecules 2001, 2, 288.
27. Garozzo, D.; Giuffrida, M.; Montaudo, G. Macromolecules 1986, 19, 1643.
28. Nealy, D. L.; Adams, L. J. J Polym Sci Part A-1: Polym Chem 1971, 9, 2063.
29. Zimmerman, H.; Kim, N. T. Polym Eng Sci 1980, 20, 680.
30. Dzieciol, M.; Trzeszczynski, J. J Appl Polym Sci 1998, 69, 2377.
31. Edge, M.; Allen, N. S.; Wiles, R.; McDonald, W.; Mortlock, S. V. Polymer 1995, 36, 227.
32. Zimmermann, H. In Developments in Polymer Degradation; Grassie, N., Ed.; Applied Science: London, 1987; Vol. 7, p 35.
33. McNeill, I. C.; Bounekhel, M. Polym Degrad Stab 1991, 34, 187.
34. Passalacqua, V.; Pilati, F.; Zamboni, V.; Fortunato, B.; Manaresi, P. Polymer 1976, 17, 1044.
35. Flynn, J. H.; Wall, L. A. Polym Lett 1966, 4, 323.
36. Ozawa, T. Bull Chem Soc Jpn 1965, 38, 1881.
37. Doyle, C. J Appl Polym Sci 1961, 5, 285.
38. Coats, A.; Redfern, J. Nature 1964, 20, 168.
39. Criado, J.; Malek, J.; Ortega, A. Thermochim Acta 1998, 147, 377.
40. Nunez, L.; Fraga, F.; Nuñez, M. R.; Villanueva, M. Polymer 2000, 41, 4635.
41. Tang, W.; Liu, Y.; Zhang, C. H.; Wang, C. Thermochim Acta 2003, 40, 839.
42. Kissinger, H. F. Anal Chem 1957, 29, 1702.
43. Gotor, F. J.;. Criado, J. M.; Malek, J.; Koga, N. J Phys Chem A 2000, 104, 1077.
44. Pérez-Maqueda, L. A.; Criado, J. M.; Gotor, F. J.; Málek, J. J Phys Chem A 2002, 106, 2862.
45. Wanjun, T.; Yuwen, L.; Hen, Z.; Zhiyong, W.; Cunxin, W. J Therm Anal Cal 2003, 74, 309.
46. Tang, W.; Liu, Y.; Yang, X.; Wang, C. Ind Eng Chem Res 2004, 43, 2054.
47. Vyazovkin, S. Thermochim Acta Part C 2000, 355, 155.